Integration of Carbon and Nitrogen Metabolism with Energy Production Is Crucial to Light Acclimation in the Cyanobacterium Synechocystis[1][W][OA]

Abhay K. Singh, Thanura Elvitigala, Maitrayee Bhattacharyya-Pakrasi, Rajeev Aurora, Bijoy Ghosh, and Himadri B. Pakrasi*

Department of Biology (A.K.S., M.B.-P., H.B.P.), Department of Electrical and Systems Engineering (T.E.), and School of Engineering (H.B.P.), Washington University, St. Louis, Missouri 63130; Department of Molecular Microbiology and Immunology, Saint Louis University School of Medicine, St. Louis, Missouri 63104 (R.A.); and Department of Mathematics and Statistics, Texas Tech University, Lubbock, Texas 79409 (B.G.)

Light drives the production of chemical energy and reducing equivalents in photosynthetic organisms required for the assimilation of essential nutrients. This process also generates strong oxidants and reductants that can be damaging to the cellular processes, especially during absorption of excess excitation energy. Cyanobacteria, like other oxygenic photosynthetic organisms, respond to increases in the excitation energy, such as during exposure of cells to high light (HL) by the reduction of antenna size and photosystem content. However, the mechanism of how Synechocystis sp. PCC 6803, a cyanobacterium, maintains redox homeostasis and coordinates various metabolic processes under HL stress remains poorly understood. In this study, we have utilized time series transcriptome data to elucidate the global responses of Synechocystis to HL. Identification of differentially regulated genes involved in the regulation, protection, and maintenance of redox homeostasis has offered important insights into the optimized response of Synechocystis to HL. Our results indicate a comprehensive integrated homeostatic interaction between energy production (photosynthesis) and energy consumption (assimilation of carbon and nitrogen). In addition, measurements of physiological parameters under different growth conditions showed that integration between the two processes is not a consequence of limitations in the external carbon and nitrogen levels available to the cells. We have also discovered the existence of a novel glycosylation pathway, to date known as an important nutrient sensor only in eukaryotes. Up-regulation of a gene encoding the rate-limiting enzyme in the hexosamine pathway suggests a regulatory role for protein glycosylation in Synechocystis under HL.

All organisms require carbon (C), nitrogen (N), phosphorus, and sulfur (S) as macronutrients for growth and development. Reduced C is essential both as building blocks in metabolic reactions and as energy sources for all organisms. Photosynthetic organisms generate reduced C through photosynthesis. These organisms use solar energy to generate chemical energy and reducing power to fix atmospheric C and assimilate other nutrients. Thus, light represents an essential nutrient for these organisms. Light also represents a significant problem for the photosynthetic organisms since duration and changes in the quality and quantity of light energy perceived by these organisms is unavoidable under natural conditions. When light perceived by photosynthetic organisms cannot be completely utilized for downstream processes, it leads to a redox imbalance and an excessive production of damaging reactive oxygen species (ROS; Apel and Hirt, 2004; Scheibe et al., 2005). Integrating nutrient-specific pathways is therefore vital to survival under constantly changing environmental and metabolic cues. It has been suggested that photosynthetic organisms accomplish this integration by tightly connecting photosynthetic processes to other principal metabolic pathways (Wang et al., 2003; Forchhammer, 2004; Gutierrez et al., 2007). For example, C and N metabolism are sinks for ATP and reducing power produced during photosynthesis. Protein complexes involved in the photosynthetic processes are in themselves a major metabolic sink for iron, S, N, and C. Similarly, intermediates of C and N metabolic pathways influence many other processes, including photosynthesis. Furthermore, photosynthetic processes capacitate several interconnected redox molecules that act as sensors for a number of metabolic pathways (Dietz, 2003; Apel and Hirt, 2004; Scheibe et al., 2005).

Genome-wide transcriptional investigations have greatly aided the understanding of molecular mecha-

nisms by which photosynthetic organisms adapt to fluctuations of environmental and metabolic cues. Recent studies in higher plants have revealed the existence of complex, interconnected regulatory and signaling networks. These networks allow them to fine tune growth and development in response to environmental and metabolic cues (Wang et al., 2003; Gutierrez et al., 2007). In contrast, existence of such regulatory and signaling networks in cyanobacteria has not been fully appreciated at global levels. However, studies limited to a few genes have shown a close relationship between principal pathways in cyanobacteria (Forchhammer, 2004). In particular, two DNA microarray studies have reported on the response of *Synechocystis* sp. PCC 6803 (*Synechocystis* hereafter) to high light (HL; Hihara et al., 2001; Huang et al., 2002). However, an understanding of responses as inferred by these studies has remained inconclusive, in part because of technological issues. For example, Hihara et al. (2001) reported that approximately 2,500 of 3,079 genes showed signal intensities that were lower than background fluorescence level or signal intensities of negative control spots. As a result, many important regulatory and structural genes could not be comprehensively identified. Recently, the time series data generated by Hihara et al. (2001) in response to HL was used to generate a gene coexpression network (Aurora et al., 2007). Such analysis revealed that when light and C are in excess, S becomes the key limiting nutrient for these organisms.

We have utilized a DNA microarray chip developed using Agilent technology that offers significant improvements in data generation. Such improvements have allowed us to confidently identify gene transcripts, including those present in low abundance. We have utilized these DNA chips to understand the response of *Synechocystis* to HL at ambient CO_2 (i.e. 0.04%). Growth and treatment conditions used in this study are significantly different compared to Hihara et al. (2001), where 1% CO_2 was used for growth and HL treatment of *Synechocystis*. The differences in cells grown under dissimilar CO_2 concentrations would be expected to have a significant impact on the response of *Synechocystis* to HL. It has been shown that cells grown in the presence of high CO_2 have a lower PSI/PSII ratio compared to air-grown cells (Satoh et al., 2002). This is a critically important physiological modification because a known HL adaptation mechanism in *Synechocystis* is to decrease the PSI/PSII ratio (Hihara et al., 1998). Our results show that *Synechocystis* grown in the presence of 0.04% CO_2 responds to excess excitation energy by reducing antenna size and photosystem content similar to *Synechocystis* treated with HL in the presence of 1% CO_2, as reported by Hihara et al. (2001). In addition, we found an intricate coordination between energy production and energy consumption processes. We have also discovered the presence of a hexosamine signaling (HS) pathway in *Synechocystis*.

RESULTS

Physiological Response of *Synechocystis* to HL

Absorption of photons by pigments associated with PSII elevates them to an electronic excited state. These pigments return to the ground state primarily via three routes (Fig. 1A). Measurement of fluorescence from cells under a given condition can be used to gather real-time information on the status of the photosynthetic process. One such measurement is the determination of the ratio of variable fluorescence to maximal fluorescence (F_v/F_m), which is interpreted as a measure of maximal quantum efficiency of PSII photochemistry. When cells grown at low light (LL) were transitioned to HL, the F_v/F_m ratio declined rapidly
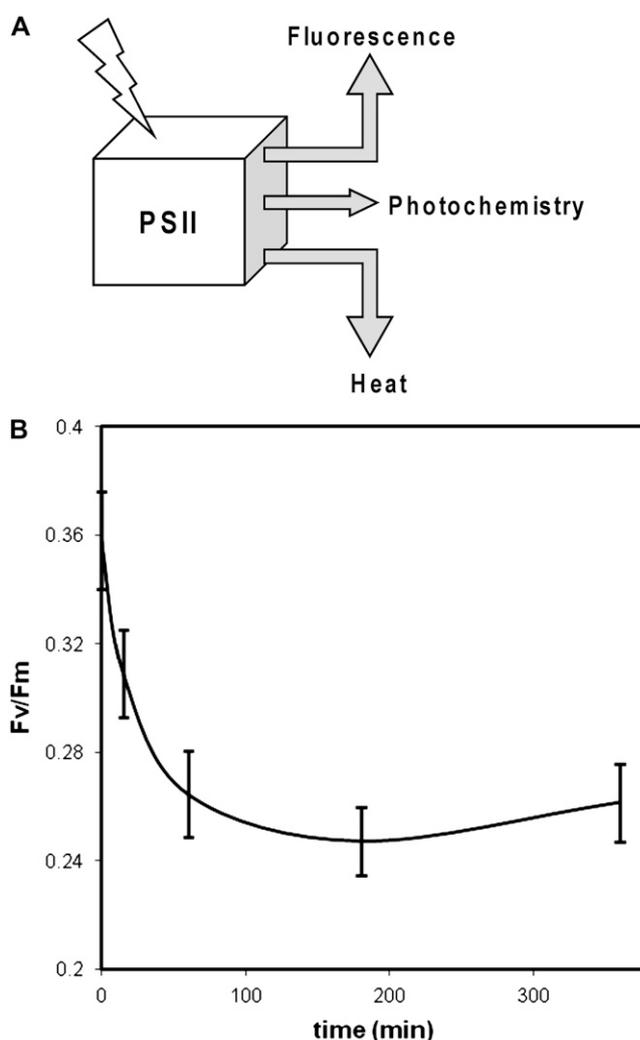

Figure 1. A, Schematic diagram showing events following absorption of light by PSII. The excitation energy absorbed by pigments associated with PSII is released primarily via three routes, either as heat, fluorescence, or utilized for photochemistry. B, Time course of changes in F_v/F_m ratios following HL treatment. *Synechocystis* cells grown at LL (30 μE m^{-2} s^{-1}) were transitioned to HL (300 μE m^{-2} s^{-1}). Temperature was maintained at 30°C during growth and treatment. Samples were withdrawn at indicated time period and fluorescence was measured in FL100.

and remained low up to 3 h (Fig. 1B). By 6 h of HL treatment, the F_v/F_m ratio began to increase and a significant increase in the F_v/F_m ratio was observed during further HL treatment (data not shown). These results suggest that photodamage to photosynthetic complexes occurs immediately upon transition to HL and recovery could be observed by 6 h under our experimental conditions. Therefore, we sampled cells up to 6 h following HL treatment as they appear to have attained homeostasis by 6 h.

Summary of Genes Regulated by HL

An overview of the impact of HL on gene regulation for various functional categories is provided in Supplemental Table S1. In total, 762 genes showed differential regulation in response to HL that differed by at least 1.3-fold ($P < 0.01$). The fold change of 1.3× was experimentally verified using real-time PCR and, combined with the *P*-value determinants, can be confidently used as criteria to identify differential regulation of a gene (Supplemental Table S2). We attribute the confidence in a 1.3-fold cutoff to the significant improvement in data generation by using the custom-designed Agilent chips. A comparative analysis of differentially regulated genes obtained in this work with those identified by Hihara et al. (2001; Table I) showed that 638 regulated genes, including 277 genes designated as hypothetical or unknown in Cyanobase, were uniquely identified in this work; 124 regulated genes were identified in both studies, although some genes showed opposite regulation, whereas only 36 regulated genes, including 23 genes designated as hypothetical or unknown in Cyanobase (http://bacteria.kazusa.or.jp/cyano), were uniquely identified by Hihara et al. (2001). In addition, several genes present on various plasmids were strongly transcribed (Supplemental Fig. S2) and differentially regulated in response to HL (Fig. 2; Supplemental Table S3). The large number of uniquely identified genes, as well as the identification of transcripts from plasmids in this work, can be attributed directly to improvements in chip design and data generation. A number of differentially regulated genes showed statistically significant differences in the fold change depending on the probe's location on an individual open reading frame (ORF; Supplemental Fig. S3), suggesting that mRNA turnover plays a role in gene regulation during HL treatment. A large number of genes showed differential regulation immediately in response to HL that increased over 4 h and eventually decreased by 6 h (Supplemental Table S1). Thus, differential regulation of genes corresponded to the physiological response of *Synechocystis* observed by the F_v/F_m ratio in response to HL.

Cluster Analysis of Differentially Regulated Genes Using Discretized Expressions

Coregulated genes were clustered using discretized expressions that have many advantages over traditional clustering methods (see "Materials and Methods"). Overall, differentially regulated genes were grouped into 11 unique clusters that showed time-dependent patterns of regulation (Fig. 2). In addition, there were 31 genes (approximately 4% of selected genes) that could not be grouped into any of 11 unique clusters. Genes present in cluster 1 (290 genes, i.e. approximately 38% of selected genes), cluster 2 (94 genes, i.e. approximately 12% of selected genes), and cluster 3 (50 genes, i.e. approximately 6% of selected genes) were down-regulated following 15 min, 1 h, and 2 h of HL treatment, respectively. Genes present in cluster 4 (29 genes, i.e. approximately 4% of selected genes) transiently decreased at 15 min and returned to initial levels by 1 h in response to HL. Genes in cluster 5 (19 genes, i.e. approximately 3% of selected genes) and cluster 6 (38 genes, i.e. approximately 5% of selected genes) were down-regulated following 15 min and 1 h of HL treatment, respectively, but returned to initial levels by 6 h. Genes present in cluster 7 (11 genes, i.e. approximately 1% of selected genes) transiently decreased, but increased following 1 h in response to HL and remained high. Genes present in cluster 8 (105 genes, i.e. approximately 14% of selected genes), cluster 9 (33 genes, i.e. approximately 4% of selected genes), and cluster 10 (24 genes, i.e. approximately 3% of selected genes) were up-regulated following 15 min, 1 h, and 2 h of HL treatment, respectively. Genes in cluster 11 (38 genes, i.e. approximately 5% of selected genes) transiently increased at 15 min, but returned to initial levels by 1 h in response to HL treatment.

It is apparent from these cluster analyses that large numbers of genes are down-regulated, suggesting that negative regulation of gene expression is a major response to HL in *Synechocystis*. Importantly, genes involved in the specific functions followed similar regulatory patterns (Supplemental Table S3). However, in a few cases, genes belonging to a given pathway are present in different clusters because of the differing patterns of regulation. For example, the *psbA* gene coding for the D1 protein of PSII was up-regulated in response to HL compared to down-regulation of other PSII genes (Supplemental Fig. S4). The increased expression of the *psbA* gene is related to increased photodamage of D1 protein caused by the over-reduction of components involved in the electron transport chain. Similarly, two genes, IF7 and IF17, involved in the inhibition of Gln synthase (GS) type I activity (Garcia-Dominguez et al., 1999) were up-regulated compared to down-regulation of other genes involved in N assimilation (Supplemental Table S3).

Regulation of Genes Encoding Proteins Involved in the Photosynthetic Process

Genes encoding proteins involved in the photosynthetic process were mostly down-regulated in response to HL (Fig. 3; also see Supplemental Table S3). A similar response was also reported by Hihara et al. (2001), suggesting that regulation of these genes

Table I. *Effects of excess C and N on the response of Synechocystis to HL treatment*

Cells were grown under normal photoautotrophic growth conditions for 24 h and diluted in fresh BG11 to bring the cell density to approximately 5×10^7 cells/mL. The indicated nutrient was added and cells were grown either under LL or HL. F_V/F_m ratios and growth rates at any given time points were measured as described in "Materials and Methods." The values are mean of three independent experiments. nd, Not determined.

	BG11		BG11 + HCO$_3^-$		BG11 + NO$_3$		BG11 + HCO$_3^-$ + NO$_3$		BG11 + 3% CO$_2$		BG11[a] + 3% CO$_2$		BG11[b] + HCO$_3^-$	
	F_V/F_m	cells/mL[b]	F_V/F_m	cells/mL	F_V/F_m	cells/mL	F_V/F_m	cells/mL	F_V/F_m	cells/mL	F_V/F_m	cells/mL	F_V/F_m	cells/mL
LL														
30 min	0.46	3.90	0.45	1.30	0.45	2.10	0.45	3.80	0.47	2.60	nd	nd	nd	nd
3 h	0.45	2.70	0.45	3.80	0.44	2.40	0.45	4.70	0.48	4.90	nd	nd	nd	nd
6 h	0.42	4.40	0.43	11.00	0.40	4.40	0.42	4.90	0.46	13.30	nd	nd	nd	nd
24 h	0.42	12.00	0.37	17.00	0.41	11.00	0.34	22.00	0.48	21.20	nd	nd	nd	nd
30 h	0.41	21.00	0.37	30.00	0.40	21.00	0.34	34.00	0.48	37.10	nd	nd	0.38	nd
HL														
30 min	0.28	4.60	0.26	4.60	0.26	3.80	0.26	4.10	0.26	5.71	0.33	4.33	0.23	7.11
3 h	0.29	4.30	0.26	5.10	0.27	4.70	0.28	3.70	0.22	5.61	0.32	5.5	0.26	6.55
6 h	0.34	6.00	0.31	7.40	0.32	4.90	0.33	4.80	0.27	7.83	0.39	10.56	0.31	7.40
24 h	0.44	21.00	0.45	22.00	0.39	22.00	0.43	23.00	0.43	23.67	0.45	34.55	0.45	24.8
30 h	0.45	27.00	0.46	31.00	0.37	30.00	0.43	32.00	0.49	nd	0.48	nd	0.48	nd

[a] Cells were adapted for 30 h under the respective conditions. [b] Cells/mL is represented as ($\times 10^7$).

in response to HL is independent of the concentration of inorganic C present during the growth and treatment of *Synechocystis*. However, we found that the number of genes differentially regulated in response to HL was much greater than that reported by Hihara et al. (2001). For example, among genes coding for PSII, a total of 18 genes were regulated, all of which, except the *psbA* gene, were down-regulated (Supplemental Fig. S4). The *psbEFLJ* operon required for PSII activity (Pakrasi et al., 1988; Lind et al., 1993; Ikeuchi et al., 1995; Regel et al., 2001) was significantly down-regulated in response to HL. Our results show that the *psb27* and *psb28* genes coding for proteins present in PSII (Kashino et al., 2002) were also down-regulated in response to HL. Similarly, all genes encoding components of PSI, except for *ycf3* and *ycf4* genes required for PSI biogenesis (Boudreau et al., 1997), were down-regulated (Supplemental Fig. S4). In contrast to Hihara et al. (2001), we found that the *psbX* gene and both *psaK* genes are down-regulated in response to HL. A major difference between the two studies was observed in the regulation of genes encoding ATP synthase. Our microarray results show that all genes encoding ATP synthase (Fig. 3) were significantly down-regulated compared to a lack of differential regulation for these genes as observed by Hihara et al. (2001).

Genes encoding phycobilisome proteins and those involved in pigment biosynthesis were down-regulated in parallel with a down-regulation of photosystem genes (Fig. 3). We observed that genes coding for phycocyanin, allophycocyanin, and the linker proteins were all down-regulated to similar extents in response to HL (Supplemental Fig. S4). This is in contrast to the report by Hihara et al. (2001), who found that *cpc* genes were down-regulated to a greater degree than the *apc* genes, perhaps to preferentially downsize the antenna size. The differences observed in the regulation of *cpc* and *apc* genes could be related to different inorganic C concentrations used for growth and HL treatment in the two

studies. Similarly, we found that genes involved in the pigment biosynthesis pathway were regulated into two distinct segments. Genes coding for proteins involved in conversion of L-Glu to δ-aminolevulinate were down-regulated, whereas those coding for proteins involved in the conversion of δ-aminolevulinate to protoporphyrin IX were not regulated. Finally, key genes involved in the conversion of protoporphyrin IX to chlorophyll and bilins were down-regulated. A similar regulation of genes coding for proteins involved in pigment biosynthesis has been observed previously (Singh et al., 2003).

Coordinated Regulation of Genes Involved in C and N Metabolism

Genes coding for Rubisco, CO$_2$-concentrating mechanism proteins, and proteins involved in glycolysis were down-regulated in response to HL. In contrast, we found significant up-regulation of genes encoding transporters involved in C transport (Fig. 3). This included both BCT1 and SbtA transporters that are known to be induced under C-limiting conditions (Wang et al., 2004). BCT1 is a high-affinity HCO$_3^-$ transporter encoded by the *cmpABCD* operon (Omata et al., 1999; Wang et al., 2004), whereas SbtA is a Na$^+$-dependent HCO$_3^-$ uptake transporter (Shibata et al., 2002). Regulation of the *sbtA* gene along with a nearby *slr1513* gene showed an interesting pattern; it increased significantly during the initial 15 min of HL treatment followed by down-regulation of both genes, which increased again by 6 h. We also found that the *ndhD3*, *ndhF3*, and *cupA* genes encoding for proteins involved in high-affinity CO$_2$ transport were up-regulated (Klughammer et al., 1999; Ohkawa et al., 2002). Interestingly, *ndhD3* and *ndhF3* genes were up-regulated for the entire duration of HL treatment, whereas the *cupA* gene was up-regulated immediately and showed an oscillating pattern.
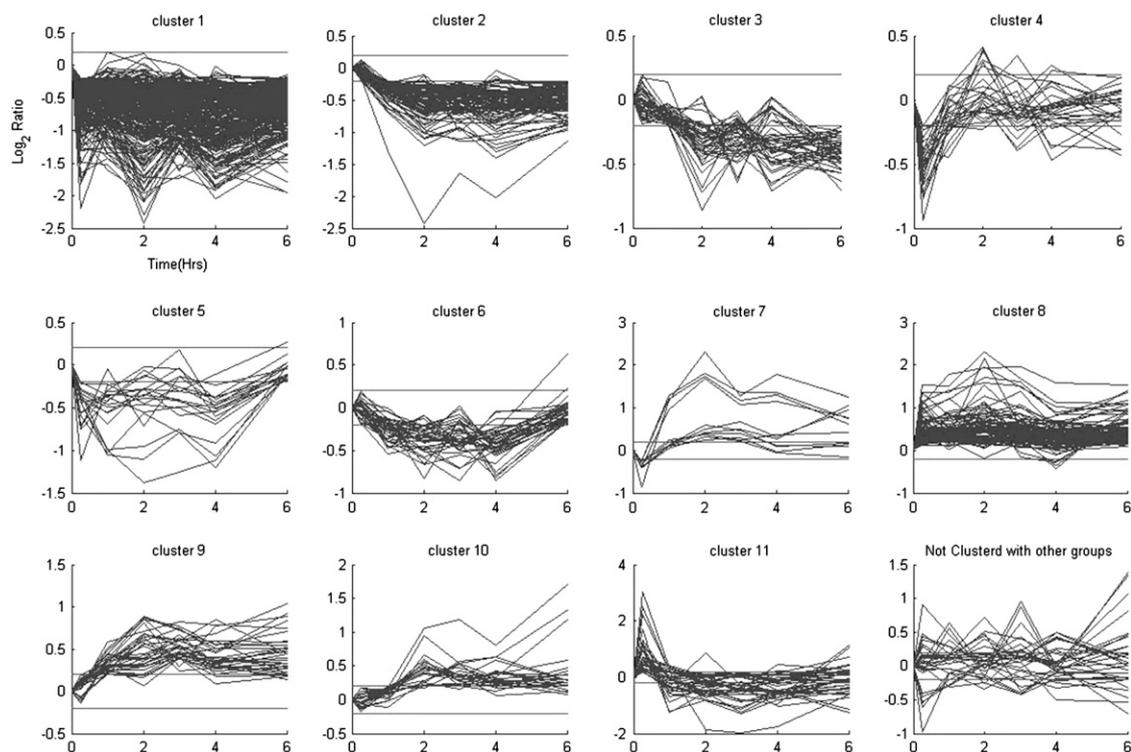
Figure 2. Distinct groups of differentially regulated genes in response to HL as revealed by clustering. The differentially regulated genes were clustered using discretized expressions as described in "Materials and Methods." The characteristics of each cluster are described in the text and genes present in various clusters are provided in Supplemental Table S3 along with their functional roles and fold change at each time point. The two solid lines in each cluster represent the fold-change cutoff (+0.3785 to −0.3785).

Regulation of genes involved in the assimilation of N by *Synechocystis* during HL treatment showed an integrated response with genes involved in CO_2 fixation (Fig. 3). Genes encoding for proteins involved in nitrate assimilation and transport (*nrt* operon), as well as ammonium and urea transport, were down-regulated in response to HL. In addition, several genes involved in the GS-GOGAT pathway were also regulated. GS combines Glu and ammonia to generate Gln using ATP produced by photosynthesis. GOGAT combines Gln produced in the first step of the pathway with 2-oxoglutarate to produce two glutamates. *glnA* and *glnN* genes encoding subunits of GS were down-regulated in response to HL. In contrast, *glsF* and *gltB*, which encode GOGAT, were not regulated in response to HL, whereas the *gltD* gene encoding NADH-GOGAT was slightly down-regulated. In contrast, genes encoding IF7 and IF17 were strongly up-regulated by HL treatment. These two proteins inhibit activity of GS type I by protein-protein interaction (Garcia-Dominguez et al., 1999).

Genes Involved in the Regulation, Protection, and Maintenance of Redox Homeostasis

A number of genes coding for proteins involved in the maintenance of redox homeostasis, cellular protection, and regulation of gene expression were differ-entially controlled by HL (Fig. 3). Redoxins, such as thioredoxins (Trxs), glutaredoxins (Grxs), and perox-iredoxins, play critical roles in the cellular protection and maintenance of redox homeostasis within cells (Dietz, 2003). DNA microarray analysis shows that genes encoding TrxA and both subunits of ferredoxin-Trx reductase were down-regulated by HL treatment. In contrast, the *ntr* gene encoding the NADP-Trx reductase and the *trxM1* gene were up-regulated in response to HL (Fig. 3). Similarly, two *prx* genes, *slr1198* (*1-cys prx*) and *sll1621* (*type II prx*), were differ-entially regulated in response to HL. The *slr1992* gene encoding glutathione peroxidase-like NADPH perox-idase was up-regulated in response to HL. In addition, we found significant temporal regulation of an operon containing the *sll1159* gene in response to HL. Sll1159 contains a Cys-X-X-Cys motif and has a typical Grx domain. Two neighboring genes, *sll1158* and *sll1160*, showed a response similar to that of the *sll1159* gene.

Genes encoding chaperones, including GroELS, HtpG, DnaK, and HspA, showed temporal up-regulation in response to HL (Fig. 3). We also found that genes coding for proteases and HL-inducible proteins (HLIPs) were significantly up-regulated in response to HL. HLIPs are small proteins suggested to be involved in the photoprotection of PSI (Salem and van Waasbergen, 2004; Jantaro et al., 2006). In addition,

Figure 3. Summary of differentially regulated genes belonging to selected processes in response to HL. Regulation pattern of genes belonging to a given process is identified by the cluster numbers as identified in Figure 2. The number of genes present in each cluster is provided in the bracket. Red and green colors represent up- and down-regulation of genes, respectively. Details of differentially regulated genes are provided in Supplemental Table S3.

we found a number of genes such as *mvrA*, *slr1300*, *slr1687*, *slr1667*, *slr1668*, and *sll1894* that showed consistently strong up-regulation during HL treatment (Fig. 3). Proteins encoded by these genes contain signature motifs that are known to play important roles in cellular protection during abnormal conditions. MvrA has been suggested to protect cells against oxidative stress (Nefedova et al., 2003). The *slr1300* gene encodes a putative flavoprotein monooxygenase. Such proteins are involved in the glutathione oxidation in animal systems as well as in systemic acquired resistance in plants that correlates with an increased production of ROS (Suh et al., 1999; Mishina and Zeier, 2006). Slr1687 contains a phycobilisome lyase HEAT-like domain suggested to being involved in the degradation of phycobilisomes. The *slr1667* and *slr1668* genes are transcriptionally regulated by Sycrp1 in response to intracellular cAMP (Yoshimura et al., 2002). The *sll1894* gene encodes a riboflavin biosynthesis protein RibA. This key enzyme is part of the riboflavin metabolism pathway that converts ribulose-5-P to essential cofactors like quinone, flavin mononucleotide, and flavin adenine dinucleotide.

A number of His kinase and response regulator genes were regulated in response to HL (Supplemental Table S3). *glnB*, *ntcA*, *lexA*, and *slr2024* genes were all down-regulated in response to HL (Fig. 3). NtcA is a positive regulator of many genes involved in N assimilation, whereas PII encoded by *glnB* is considered to be a key sensor of the intracellular C/N ratio (Forchhammer, 2004). LexA has also been shown to regulate genes involved in assimilation of C and N (Domain et al., 2004). Slr2024, a response regulator belonging to the CheY family, has been found to be associated with thylakoid membranes (Wang et al., 2000). Similarly, *slr0687*, *slr1214*, and *slr2104* were up-regulated in response to HL (Fig. 3). Slr0687 was clustered with CikA in a phylogeny tree based on aligned GAF domains (Montgomery and Lagarias, 2002). CikA has been suggested to be involved in sensing the redox status of plastoquinone (PQ; Ivleva et al., 2006). Slr1214, a member of the PatA family of regulators that possess CheY-like response regulator

domains, has previously been shown to be up-regulated under C-limiting conditions (Wang et al., 2004), exposure to H_2O_2 (Li et al., 2004), and under iron-limiting conditions (Singh et al., 2003). Slr2104 contains PAS motifs in its sensor region. This motif is known to regulate light- and O_2-stimulated signaling pathways (Zhulin and Taylor, 1998).

Identification of the HS Pathway in *Synechocystis*

A single-copy gene (*sll0220*) encoding Gln:Fru-6-P amidotransferase (GFAT) was consistently up-regulated throughout HL treatment (cluster 8). GFAT catalyzes the formation of glucosamine-6-P from Fru-6-P (Fig. 4). It is the rate-limiting enzyme of the HS pathway, which is required for *O*-glycosylation of soluble proteins in eukaryotes and in some bacteria (Love and Hanover, 2005). A branch-point metabolite, UDP-*N*-acetyl-ᴅ-glucosamine (UDP-GlcNAc), produced in this pathway can either be utilized for the biosynthesis of peptidoglycan or can act as a substrate for *O*-linked GlcNAc transferase (OGT; Fig. 4). However, our data show that several genes involved in the biosynthesis of peptidoglycan were down-regulated in response to HL (Fig. 4). These results suggest that increased synthesis of UDP-GlcNAc as inferred by up-regulation of the *GFAT* gene is utilized by OGT for the addition of GlcNAc to substrate proteins. It is known that OGT glycosylates its substrates by responding to concentrations of UDP-GlcNAc (Love and Hanover, 2005). We further confirmed differential regulation of the *GFAT* gene during HL treatment by reverse transcription (RT)-PCR (Fig. 5A). Interestingly, steady-state transcript levels of the *GFAT* gene in control samples decreased with time, whereas cells transitioned to HL maintained steady-state transcript levels of the *GFAT* gene for the entire duration of HL treatment. We also found that *Synechocystis* contains at least two OGT proteins. An OGT encoded by the *slr0626* gene shows similarity to GmaR, a recently identified OGT in *Listeria monocytogenes* (Shen et al., 2006). A second OGT encoded by the *slr1816* gene shows similarity with SPINDLY, an OGT present in *Arabidopsis*

thaliana, which is involved in GA-dependent signal transduction (Jacobsen et al., 1996). Additional evidence on the presence of HS pathway in *Synechocystis* comes from an identification of glycosylated proteins with monoclonal antibody CTD110.6 (Fig. 5C). The CTD110.6 antibody specifically recognizes *O*-linked GlcNAc residues (Comer et al., 2001). Four major proteins of apparent molecular mass 21, 25, 28, and 34 kD were detected by the CTD110.6 antibody on a western blot (Fig. 5C). In addition, several minor proteins of higher molecular mass could also be detected. It is clear from the comparison between the western blot and a Coomassie-stained SDS-polyacrylamide gel (Fig. 5B) that proteins identified by CTD110.6 are due to specific interactions because they do not belong to bands representing abundant proteins. These results together suggest that the HS pathway is present and active in *Synechocystis*. Furthermore, regulation of the gene for the rate-limiting enzyme GFAT by HL treatment suggests that the HS pathway may act as a regulatory pathway in *Synechocystis* as shown in eukaryotes (Love and Hanover, 2005).

Response of *Synechocystis* to HL in the Presence of Excess Nutrients

The results presented in this work from DNA microarray experiments suggest that *Synechocystis* cells limit the assimilation of C and N during initial HL treatment. To rule out the possibility that key nutrients were not limiting, we measured growth rates and F_v/F_m ratios in response to HL in the presence of excess C and N added just before HL treatment, as well as in cells preadapted to growth in BG11 medium supplemented either with 10 mM HCO_3^- or 3% CO_2 (Table I). The growth rates and F_v/F_m ratios measured in the presence of 10 mM HCO_3^-, 50 mM NO_3^-, or 3% CO_2 during HL treatment were indistinguishable from HL-treated cells grown in air. Under all growth conditions, the F_v/F_m ratio decreased during the first 30 min of HL treatment and a recovery could be seen by 6 h, which was completed by 24 h. In contrast, cells adapted to 10 mM HCO_3^- or 3% CO_2 responded differently to HL. The F_v/F_m ratio in cells adapted to 3% CO_2 decreased to a lesser extent and recovery was faster as compared to air-grown and HCO_3^--adapted cells. The HCO_3^--adapted cells appeared to be more sensitive to HL and their response was similar to air-grown cells. Moreover, cells adapted to 3% CO_2 showed faster growth during HL treatment similar to the growth rates as reported by Hihara et al. (2001). These results show that the initial adaptation of *Synechocystis* to HL is independent of the presence of excess C and N. Furthermore, the responses of HCO_3^-- and 3% CO_2-adapted cells to HL suggest that an adjustment of PSII and PSI stoichiometry is a key adaptive mechanism. It is known that cells grown in HCO_3^- or excess CO_2 have higher and lower PSI/PSII ratios, respectively, compared to air-grown cells (Satoh et al., 2002). Since the most important physiological adaptation in photosynthetic cells during HL is to lower PSI/PSII ratio (Hihara et al., 1998), it would appear that cells grown in 3% CO_2 have undergone an adaptation that is otherwise only observed during the first few hours of HL treatment in air-grown cells.

DISCUSSION

In this study, we have combined transcriptome data with measurements of physiological parameters under different growth conditions to elucidate global physiological responses to HL in *Synechocystis*. Figure 6 describes the coordination between pathways inferred from the transcriptome data during HL treatment in *Synechocystis* at ambient CO_2 concentration. *Synecho-*
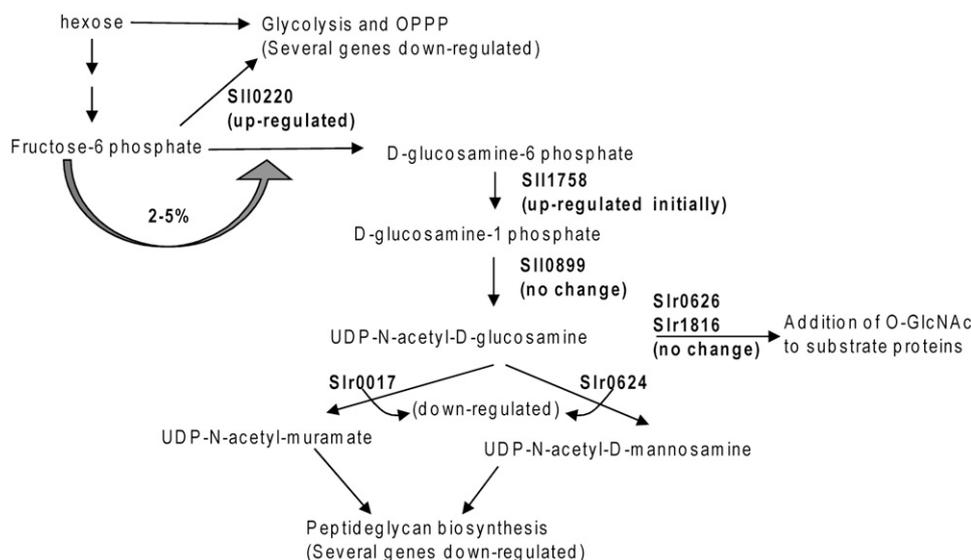

Figure 4. Schematic diagram of the HS pathway in *Synechocystis*. Genes involved in the pathway have been listed along with their regulation by HL treatment.
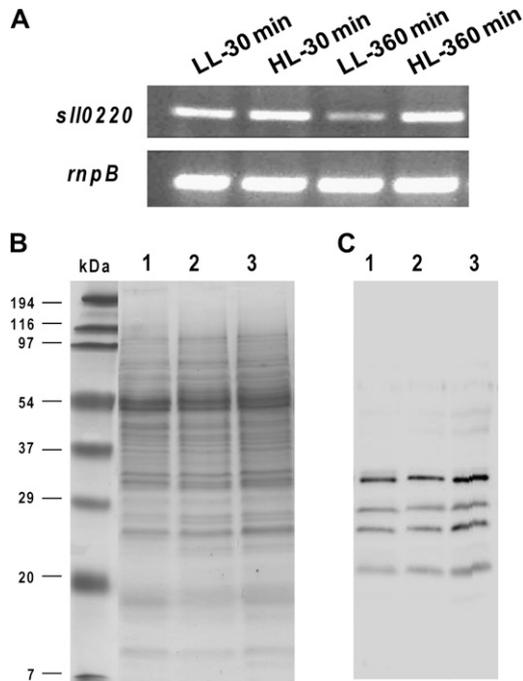
A

B **C**

Figure 5. A, RT-PCR of the *GFAT* gene. *Synechocystis* cells were treated with HL for indicated time periods. Total RNAs were isolated and RT-PCR was performed as described in "Materials and Methods." B and C, Coomassie-stained SDS-polyacrylamide gel (B) and western-blot analysis (C) of total cell extracts isolated from *Synechocystis* grown under various light conditions using CTD110.6 against O-GlcNAc. *Synechocystis* cells were grown in BG11 medium at 5 μE m^{-2} s^{-1} (lane 1); 30 μE m^{-2} s^{-1} (lane 2); and 200 μE m^{-2} s^{-1} for 24 h (lane 3).

cystis, with its large content of photosystems and antenna size to maximize light absorption under LL growth conditions, undergoes photodamage during HL treatment as revealed by F_v/F_m ratios. This photodamage is a result of the accumulation of reduced components involved in electron transport due to the increased excitation by HL and not because of the presence of limited amounts of CO_2 that could intimately lead to the accumulation of reduced components. This is also apparent from results indicating that presence of HCO_3^- or 3% CO_2 during HL treatment had similar effects on growth rates and F_v/F_m ratios as cells under 0.04% CO_2. Cells adjust to HL by down-regulating genes coding for PSII, PSI, phycobilisome, ATP synthase, and genes involved in pigment biosynthesis. Down-regulation of these genes corresponds with the well-known physiological mechanism that reduction in photosystem content is a mechanistically key adaptive response to prevent over-reduction of components involved in the electron transport chain. An immediate consequence of this photodamage is a decreased output of products from the light reactions.

The limited energy production during the initial period of HL treatment affected the ability of cells to fix CO_2. This was evident from the down-regulation of genes encoding CO_2-concentrating mechanism proteins and Rubisco. The reduced CO_2 fixation triggered

an integrated homeostatic response in the assimilation of N and led to the down-regulation of genes involved in N transport, assimilation, and regulation. In cyanobacteria, two proteins, PII and NtcA, control N assimilation (Forchhammer, 2004). It has been suggested that PII links the state of a central C and energy metabolite to the control of N assimilation by sensing 2-oxoglutarate and ATP (Muro-Pastor et al., 2001; Forchhammer, 2004). It is also known that assimilated C in *Synechocystis* is eventually channeled into 2-oxoglutarate because of an incomplete TCA cycle that solely functions in N assimilation. We, therefore, suggest that limited CO_2 fixation during HL treatment leads to reduced N assimilation. Indeed, N was not limiting under our experimental conditions because the addition of excess N did not help to restore the growth of cells during HL treatment. Thus, it appears that cells invoked a homeostatic response by limiting the assimilation of N. The lesser assimilation of C and N had downstream consequences on various pathways, including those involved in transcription, translation, DNA replication, fatty acid metabolism, and biosynthesis of amino acid and nucleotides (Fig. 3).

Our transcriptome data also showed that cells maintain redox poise during HL by differential regulation of key genes coding for peroxiredoxins, Grxs, Trxs, MvrA, and flavoprotein monooxygenase. Whereas some of these may simply be involved in maintaining the redox poise, others may also act as redox-dependent signaling. Up-regulation of a gene coding for a putative flavoprotein monooxygenase is particularly intriguing. This protein has been suggested to be a vital component of redox machinery of cells involved in the oxidation of a variety of thiols, including GSH, Cys, and cysteamine using molecular oxygen and NADPH in yeast (Suh et al., 1999), and also in relation to the production of ROS in plants (Mishina and Zeier, 2006). Furthermore, regulation of Trxs and their partner
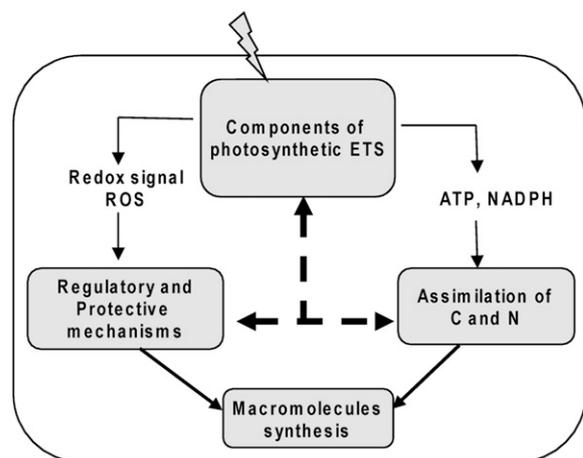

Figure 6. Schematic model of HL response in *Synechocystis*. Black arrows indicate the sequence in which HL impacts metabolic pathways. Broken arrows indicate the integration of responses that have interdependent impact on each other.

reductases could play a key role in signaling during HL. For example, TrxA has been shown to be involved in the light-induced redox regulation of proteins involved in the assimilation and storage of C and N in *Synechocystis* (Lindahl and Florencio, 2003). Because the reduction state of Trx has a stimulatory effect on anabolic processes, down-regulation of *trxA* and *ftr* and perhaps their activity during HL would signal availability of light energy. Thus, it appears that, together with PII and NtcA, TrxA may interact in a multidimensional network to control proteins involved in the assimilation of C and N. Interestingly, genes coding for TrxM and NTR were up-regulated during HL. Whereas the significance and targets of TrxM in *Synechocystis* are unknown, its up-regulation during HL would suggest a role in activation of proteins that may be involved in the adaptation mechanism. In addition, up-regulation of *ntr* would suggest a potential interaction between TrxM and NTR.

It appears that *Synechocystis* responds to HL by utilizing multiple regulatory inputs that interact in a multidimensional network to regulate gene expression required to maintain the homeostasis of various metabolic pathways (Fig. 6). The existence of such a regulatory network is evident from the regulation of PII, TrxA, and LexA. All three proteins have been shown to regulate enzymes involved in pathways leading to the assimilation of C and N (Lindahl and Florencio, 2003; Domain et al., 2004; Forchhammer, 2004). The main signal inputs appear to be the redox state of PQ, ferredoxin, and H_2O_2. Although our data do not differentiate whether these regulatory inputs act simultaneously or there exists a temporal separation, it is clear that all three play a role in C and N assimilation. PQ has been suggested to be a key redox signal for the distribution of absorbed excitation energy between photosystems and expression of several genes (Pfannschmidt, 2003). In this regard, sensing of PQ redox state by PII (Hisbergues et al., 1999) could be an important regulatory signal toward the maintenance of balanced ratios between C and N. Whether there are other sensors and regulators that respond to the redox state of PQ or elevated production of H_2O_2 remains to be seen, although our transcriptome data did identify a number of such genes, including *slr0687*, *slr2024*, and *slr2104*. These genes have the potential to be involved in the redox signaling linked to the photochemistry (Zhulin and Taylor, 1998; Wang et al., 2000; Montgomery and Lagarias, 2002; Ivleva et al., 2006). Such proteins may act independently or as part of an integrated redox signal-processing system that disseminates information via posttranslational modifications, ultimately leading to gene expression. In this regard, presence of the HS pathway involved in *O*-glycosylation of substrate proteins in *Synechocystis* offers an additional regulatory mechanism. Glycosylation of soluble proteins is considered a key regulatory mechanism in eukaryotes. Such modification occurs at phosphorylation sites in substrate proteins, which, in turn, compete with the phospho-relay-based signal

transduction pathway (Love and Hanover, 2005). The fact that the rate-limiting enzyme of this pathway is up-regulated during HL suggests that the HS pathway could play a significant regulatory role during stress conditions in cyanobacteria.

In conclusion, transcriptome data presented in this study in response to HL has led us to a better understanding of integrated responses between various pathways and processes required for the maintenance of redox homeostasis during HL. Our results show that most metabolic pathways are closely linked to primary energy production (Fig. 6). This coordination between processes appears to be a result of complex networking of overlapping signaling pathways that coordinate to regulate gene expression to optimize metabolic adjustments. The identification of various candidate genes, as well as the presence of several hypothetical and unknown genes in various clusters, provides a way forward toward understanding their specific contribution during HL stress.

MATERIALS AND METHODS

Growth Conditions and HL Treatment

Synechocystis cells were grown at 30°C in BG11 medium buffered with 10 mM TES-KOH (pH 8.2) and bubbled with air. Illumination was at 30 μE m^{-2} s^{-1} (LL) provided by fluorescent cool-white lights. Cell growth was monitored by measuring OD at 730 nm on a DW2000 (SLM-AMINCO). For HL treatment, cells grown at LL were transferred in a long test tube (3 cm in diameter) to a cell density of approximately 5×10^7 cells/mL. The tubes containing cells were transferred in a thermostat water bath maintained at 30°C and illuminated with a white-light intensity of 300 μE m^{-2} s^{-1} (HL). Cells were air bubbled during HL treatment. Cells from LL- and HL-illuminated cultures were collected after 15 min, 1 h, 2 h, 3 h, 4 h, and 6 h. Cells were harvested by centrifugation at 6,000g, frozen in liquid nitrogen, and stored at −80°C.

Room Temperature Chlorophyll Fluorescence Measurement

Fluorescence induction kinetics at room temperature were performed on a dual modulation kinetic fluorometer (model FL-100; Photon Systems Instruments) interfaced with a computer.

Isolation of RNA

Total RNA from *Synechocystis* cells was isolated using RNAwiz kit (Ambion) as described by the manufacturer, with some modifications. Briefly, 1 mL of prewarmed RNAwiz at 70°C was pipetted directly into the frozen cells and mixed quickly by vortexing. Following 10-min incubation at 70°C, 0.2 mL of chloroform was added, vigorously mixed, and incubated at room temperature for 10 min. The phase separation was achieved by centrifugation (15 min, 23,000g, 4°C). The aqueous phase containing RNA was transferred in a new Eppendorf tube and an equal volume of diethyl pyrocarbonate (DEPC)-treated water was added, extracted with water-saturated phenol, and finally precipitated by the addition of equal volume of isopropanol. Subsequently, total RNA were pelleted by centrifugation (20 min, 23,000g, 4°C), washed with 75% ethanol, and resuspended in 50 μL of DEPC-treated water. The quantity and quality of extracted RNA were determined spectrophotometrically (Nanodrop) at 260 and 280 nm and by Bio-Analyzer (Agilent).

Preparation of Fluorescently Labeled Probes

Total RNA isolated from LL- and HL-treated cells was fluorescently labeled either with Cy3 or Cy5 using the MICROMAX ASAP RNA-labeling kit (Perkin-Elmer Life Sciences) according to the manufacturer's instructions.

Two micrograms of total RNA, diluted in the ASAP labeling buffer on ice to a final volume of 19 μL and 1 μL of either Cy3 or Cy5 chemical-labeling reagent, respectively, was added to the reaction mixture. The reaction mixture was incubated at 85°C for 15 min in a thermal cycler (Eppendorf). The reaction mixture was transferred to ice and 5 μL of ASAP stop solution was added to the reaction mixture. The labeled RNA was individually purified using a PCR purification spin column (Zymo Research) and eluted with 20 μL of DEPC-treated water. The specific activity of the labeled RNA was determined in a Nanodrop.

Microarray Design and Fabrication

The *Synechocystis* 11K oligo DNA microarray used in these studies was custom designed and constructed using Agilent noncontact inkjet technology (Agilent). This technology avoids the defects caused by the surface tension interaction with the microarray surface and results in the construction of microarray with more uniform and consistent features. The probes printed on these arrays are 60-mer oligomers that are known to yield excellent sensitivity and specificity compared to cDNA-based DNA microarray and 20-mer oligomer. Candidate oligonucleotides representing 3,459 genes in *Synechocystis* were selected from the 3′ end of genes. The selected probes were filtered according to optimal base-composition profiles and screened on the basis of predicted hybridization properties and potential cross-hybridization with other sequences. For genes >0.9 kb, an additional probe corresponding to the 5′ region of gene was selected. In the case of genes present on plasmids, target sequences were selected based on self-annotation (Kazusa annotation for plasmids was not available at the time of microarray design). The predicted ORFs from plasmids matched for >95% of currently annotated ORFs; some were represented by multiple oligos and some selected probes did not correspond to any ORF currently annotated in Cyanobase. We also randomly duplicated some probes to provide experimental evidence on intra-array variance. Each microarray slide consisted of two identical arrays consisting of 8,091 probes.

Hybridization, Scanning, and Data Extraction

Fluorescently labeled probes were hybridized to *Synechocystis* 11K custom oligo DNA microarrays. For each array, we mixed 700 ng of Cy3- and Cy5-labeled RNA to a final specific activity of 50 pmol/μg of RNA. Cold RNA was added to adjust the total amount of RNA to 700 ng in the case of higher specific activity of labeled probe. Hybridization, scanning, and data extraction were performed by MOgene (www.mogene.com). Hybridization and wash processes were performed according to the manufacturer's instructions (Agilent). The hybridized microarrays were scanned using an Agilent Microarray Scanner (Agilent). Feature extraction software (Agilent) was used for the image analysis and data extraction processes using parameters optimized for prokaryotic arrays. The transcriptome data generated in this work has been submitted to the ArrayExpress database at the European Bioinformatics Institute (accession no. E-TABM-333).

Experimental Design and Statistical Analysis

The experimental design used to identify differentially regulated genes in response to HL is shown in Supplemental Figure S1A. For each time point, we have used two biological replicates and each biological replicate consists of three process replicates, including a dye swap. Preparation of fluorescent-labeled probes by direct labeling of RNA avoided bias introduced by reverse transcription of mRNA and resulted in excellent signal-to-noise ratio (Supplemental Fig. S1B).

Microarray data were processed using Matlab (MathWorks). A single microarray consisted of 8,635 probes, including 544 control probes. We excluded the control probes from further analysis. The coefficient of variation (CV) of individual spots was used to quantify the intensity distribution of individual pixels categorized as signal or background. It was observed that, on average, more than 85% of spots for green channel had a CV value <10%, whereas the corresponding percentage for red channel was 70%. Furthermore, except for few spots (<10 of 8,091), a majority of spots had a CV value <20%. These results show that the pixel intensity variation within the spot was quite low. Similar results were also observed for the background. The pixel intensities obtained from a 16-bit scanner (Agilent Technologies Scanner G2505B US22502547) would be between 0 to 65,535. We observed signal intensities of the spots in the range of 100 to 65,000, suggesting that the distribution of spot intensities was very good (Supplemental Fig. S1C). Mean intensity of spots for a given chip was found to be between 1,500 to 3,200, whereas background intensities varied in the range of 40 to 50. This suggests clear separation between signal and background. In addition, very few spots contained saturated pixels. Thus, data obtained in the present study using the direct-labeling technique and DNA microarray were of high quality.

We used the local weighted linear regression (LOWESS)-based data normalization procedure for removing the intensity-based trends observed in the microarray data. It has been suggested that LOWESS performs well when there are systematic trends in the data compared to other data normalization techniques (Quackenbush, 2002). The robust version of LOWESS normalization, which is more resistant to outliers compared to the standard LOWESS algorithm, was used with a window size of 25%. Supplemental Figure S1, C and D, shows the I-R plot of a representative microarray before (C) and after (D) the normalization.

The standard t test was used to quantify the consistency of measurements across different microarrays. P value was calculated with the null hypothesis that the samples are from a distribution with zero mean. To pick differentially expressed genes, we employed two-way criteria. A gene was considered as differentially expressed if the absolute value of its $\log_2$ ratio value exceeded a particular threshold and P value was less than a given significance level at any of the time points over the observations. Due to the high quality of the data, we were able to use 1% significance level for the P-value cutoff. A threshold of ±0.3785 (i.e. ±1.3-fold change) was used as the cutoff for the log ratio. We further established using real-time PCR experiments that 1.3-fold changes reported in microarray measurements are indeed a true differential behavior of the genes (Supplemental Table S2). Under these criteria, 762 genes were identified as differentially expressed in response to HL treatment and used for further analysis.

Cluster Analysis

The main behavioral patterns within the gene expression data were identified by cluster analysis using discretized expressions. This approach offers several advantages compared to other available methods for clustering. First, it does not require specifying the number of clusters beforehand because different patterns in the data are readily observed; second, it is less sensitive to the inherent noise in the data and, finally, it can group genes with some nonlinear relations. Gene expressions at any given time points were discretized to three levels, namely, 1 if log ratio value >0.3785 (up-regulated genes), -1 if log ratio value <-0.3785 (down-regulated genes), and 0 for genes not differentially regulated, to get a discretized vector for each gene. Genes with similar vectors were grouped together and put in a cluster. After an initial phase of clustering, we combined clusters that did not show significant differences among each other. Using this approach, the differentially regulated genes were grouped in 11 clusters that showed distinct behavioral patterns of genes. Those genes which did not fall into any of these categories were combined in cluster 12 (Fig. 2).

Total Protein Extraction and Western Blotting

Total cell extracts from *Synechocystis* were isolated as described previously (Kashino et al., 2002). Proteins were electrophoresed on 16% SDS-PAGE containing 6 M urea as described previously (Kashino et al., 2002), transferred on a nitrocellulose membrane, and probed with monoclonal antibody CTD110.6 against *O*-linked GlcNAc (Covance). Proteins were visualized using a chemiluminescent detection system (Millipore).

RT-PCR

Total RNA extracted from *Synechocystis* cells exposed to different light conditions were treated with RNase-free DNase I (Invitrogen) and used for RT reaction. The cDNA was synthesized using SuperScript II (Invitrogen) and random hexamer primers. The cDNA products were amplified by PCR using gene-specific primers (Supplemental Table S2) and analyzed by electrophoresis on 2% agarose gel. The *RNase P* gene was used as a control template.

Supplemental Data

The following materials are available in the online version of this article.

Supplemental Figure S1. Experimental design for DNA microarray.

Supplemental Figure S2. Steady-state transcript level of genes found on various plasmids.

Supplemental Figure S3. mRNA decay in response to HL.

Supplemental Figure S4. Regulation of genes involved in photosynthesis.

Supplemental Table S1. Summary of differentially regulated genes.

Supplemental Table S2. Verification of DNA microarray data by quantitative PCR.

Supplemental Tables S3. List of differentially regulated genes in response to HL.

LITERATURE CITED

Apel K, Hirt H (2004) Reactive oxygen species: metabolism, oxidative stress, and signal transduction. Annu Rev Plant Biol **55**: 373–379

Aurora R, Hihara Y, Singh AK, Pakrasi HB (2007) A network of genes regulated by light in cyanobacteria. OMICS **11**: 166–185

Boudreau E, Takahashi Y, Lemieux C, Turmel M, Rochaix JD (1997) The chloroplast ycf3 and ycf4 open reading frames of Chlamydomonas reinhardtii are required for the accumulation of the photosystem I complex. EMBO J **16**: 6095–6104

Comer FI, Vosseller K, Wells L, Accavitti MA, Hart GW (2001) Characterization of a mouse monoclonal antibody specific for *O*-linked *N*-acetylglucosamine. Anal Biochem **293**: 169–177

Dietz KJ (2003) Redox control, redox signaling, and redox homeostasis in plant cells. Int Rev Cytol **228**: 141–193

Domain F, Houot L, Chauvat F, Cassier-Chauvat C (2004) Function and regulation of the cyanobacterial genes lexA, recA and ruvB: LexA is critical to the survival of cells facing inorganic carbon starvation. Mol Microbiol **53**: 65–80

Forchhammer K (2004) Global carbon/nitrogen control by PII signal transduction in cyanobacteria: from signals to targets. FEMS Microbiol Rev **28**: 319–333

Garcia-Dominguez M, Reyes JC, Florencio FJ (1999) Glutamine synthetase inactivation by protein-protein interaction. Proc Natl Acad Sci USA **96**: 7161–7166

Gutierrez RA, Lejay LV, Dean A, Chiaromonte F, Shasha DE, Coruzzi GM (2007) Qualitative network models and genome-wide expression data define carbon/nitrogen-responsive molecular machines in Arabidopsis. Genome Biol **8**: R7

Hihara Y, Kamei A, Kanehisa M, Kaplan A, Ikeuchi M (2001) DNA microarray analysis of cyanobacterial gene expression during acclimation to high light. Plant Cell **13**: 793–806

Hihara Y, Sonoike K, Ikeuchi M (1998) A novel gene, pmgA, specifically regulates photosystem stoichiometry in the cyanobacterium Synechocystis species PCC 6803 in response to high light. Plant Physiol **117**: 1205–1216

Hisbergues M, Jeanjean R, Joset F, Tandeau de Marsac N, Bedu S (1999) Protein PII regulates both inorganic carbon and nitrate uptake and is modified by a redox signal in synechocystis PCC 6803. FEBS Lett **463**: 216–220

Huang L, McCluskey MP, Ni H, LaRossa RA (2002) Global gene expression profiles of the cyanobacterium Synechocystis sp. strain PCC 6803 in response to irradiation with UV-B and white light. J Bacteriol **184**: 6845–6858

Ikeuchi M, Shukla VK, Pakrasi HB, Inoue I (1995) Directed inactivation of the psbI gene does not affect photosystem II in the cyanobacterium Synechocystis sp. PCC 6803. Mol Gen Genet **249**: 622–628

Ivleva NB, Gao T, LiWang AC, Golden SS (2006) Quinone sensing by the

circadian input kinase of the cyanobacterial circadian clock. Proc Natl Acad Sci USA **103**: 17468–17473

Jacobsen SE, Binkowski KA, Olszewski NE (1996) SPINDLY, a tetratricopeptide repeat protein involved in gibberellin signal transduction in Arabidopsis. Proc Natl Acad Sci USA **93**: 9292–9296

Jantaro S, Ali Q, Lone S, He Q (2006) Suppression of the lethality of high light to a quadruple HLI mutant by the inactivation of the regulatory protein PfsR in Synechocystis PCC 6803. J Biol Chem **281**: 30865–30874

Kashino Y, Lauber WM, Carroll JA, Wang Q, Whitmarsh J, Satoh K, Pakrasi HB (2002) Proteomic analysis of a highly active photosystem II preparation from the cyanobacterium Synechocystis sp. PCC 6803 reveals the presence of novel polypeptides. Biochemistry **41**: 8004–8012

Klughammer B, Sultemeyer D, Badger MR, Price GD (1999) The involvement of NAD(P)H dehydrogenase subunits, NdhD3 and NdhF3, in high-affinity CO_2 uptake in Synechococcus sp. PCC7002 gives evidence for multiple NDH-1 complexes with specific roles in cyanobacteria. Mol Microbiol **32**: 1305–1315

Li H, Singh AK, McIntyre LM, Sherman LA (2004) Differential gene expression in response to hydrogen peroxide and the putative PerR regulon of Synechocystis sp. strain PCC 6803. J Bacteriol **186**: 3331–3345

Lind LK, Shukla VK, Nyhus KJ, Pakrasi HB (1993) Genetic and immunological analyses of the cyanobacterium Synechocystis sp. PCC 6803 show that the protein encoded by the psbJ gene regulates the number of photosystem II centers in thylakoid membranes. J Biol Chem **268**: 1575–1579

Lindahl M, Florencio FJ (2003) Thioredoxin-linked processes in cyanobacteria are as numerous as in chloroplasts, but targets are different. Proc Natl Acad Sci USA **100**: 16107–16112

Love DC, Hanover JA (2005) The hexosamine signaling pathway: deciphering the ''O-GlcNAc code''. Sci STKE **312**: re13

Mishina TE, Zeier J (2006) The Arabidopsis flavin-dependent monooxygenase FMO1 is an essential component of biologically induced systemic acquired resistance. Plant Physiol **141**: 1666–1675

Montgomery BL, Lagarias JC (2002) Phytochrome ancestry: sensors of bilins and light. Trends Plant Sci **7**: 357–366

Muro-Pastor MI, Reyes JC, Florencio FJ (2001) Cyanobacteria perceive nitrogen status by sensing intracellular 2-oxoglutarate levels. J Biol Chem **276**: 38320–38328

Nefedova LN, Fantin Iu S, Zinchenko VV, Babykin MM (2003) The prqA and mvrA genes encoding carrier proteins control resistance to methyl viologen in the cyanobacterium Synechocystis sp. PCC6803. Genetika **39**: 336–340

Ohkawa H, Pakrasi HB, Ogawa T (2002) Two types of functionally distinct NAD(P)H dehydrogenases in Synechocystis sp. strain PCC6803. J Biol Chem **275**: 31630–31634

Omata T, Price GD, Badger MR, Okamura M, Gohta S, Ogawa T (1999) Identification of an ATP-binding cassette transporter involved in bicarbonate uptake in the cyanobacterium Synechococcus sp. strain PCC 7942. Proc Natl Acad Sci USA **96**: 13571–13576

Pakrasi HB, Williams JG, Arntzen CJ (1988) Targeted mutagenesis of the psbE and psbF genes blocks photosynthetic electron transport: evidence for a functional role of cytochrome b559 in photosystem II. EMBO J **7**: 325–332

Pfannschmidt T (2003) Chloroplast redox signals: how photosynthesis controls its own genes. Trends Plant Sci **8**: 33–41

Quackenbush J (2002) Microarray data normalization and transformation. Nat Genet **32**: 496–501

Regel RE, Ivleva NB, Zer H, Meurer J, Shestakov SV, Herrmann RG, Pakrasi HB, Ohad I (2001) Deregulation of electron flow within photosystem II in the absence of the PsbJ protein. J Biol Chem **276**: 41473–41478

Salem K, van Waasbergen LG (2004) Light control of hliA transcription and transcript stability in the cyanobacterium Synechococcus elongatus strain PCC 7942. J Bacteriol **186**: 1729–1736

Satoh A, Kurano N, Senger H, Miyachi S (2002) Regulation of energy balance in photosystems in response to changes in CO_2 concentrations and light intensities during growth in extremely-high-CO_2-tolerant green microalgae. Plant Cell Physiol **43**: 440–451

Scheibe R, Backhausen JE, Emmerlich V, Holtgrefe S (2005) Strategies to maintain redox homeostasis during photosynthesis under changing conditions. J Exp Bot **56**: 1481–1489

Shen A, Kamp HD, Grundling A, Higgins DE (2006) A bifunctional O-GlcNAc transferase governs flagellar motility through anti-repression. Genes Dev **20**: 3283–3295

Shibata M, Katoh H, Sonoda M, Ohkawa H, Shimoyama M, Fukuzawa H,

Kaplan A, Ogawa T (2002) Genes essential to sodium-dependent bicarbonate transport in cyanobacteria: function and phylogenetic analysis. J Biol Chem **277:** 18658–18664

Singh AK, McIntyre LM, Sherman LA (2003) Microarray analysis of the genome-wide response to iron deficiency and iron reconstitution in the cyanobacterium Synechocystis sp. PCC 6803. Plant Physiol **132:** 1825–1839

Suh JK, Poulsen LL, Ziegler DM, Robertus JD (1999) Yeast flavin-containing monooxygenase generates oxidizing equivalents that control protein folding in the endoplasmic reticulum. Proc Natl Acad Sci USA **96:** 2687–2691

Wang HL, Postier BL, Burnap RL (2004) Alterations in global patterns of gene expression in Synechocystis sp. PCC 6803 in response to inorganic carbon limitation and the inactivation of ndhR, a LysR family regulator. J Biol Chem **279:** 5739–5751

Wang R, Okamoto M, Xing X, Crawford NM (2003) Microarray analysis of the nitrate response in Arabidopsis roots and shoots reveals over 1,000 rapidly responding genes and new linkages to glucose, trehalose-6-phosphate, iron, and sulfate metabolism. Plant Physiol **132:** 556–567

Wang Y, Sun J, Chitnis PR (2000) Proteomic study of the peripheral proteins from thylakoid membranes of the cyanobacterium Synechocystis sp. PCC 6803. Electrophoresis **21:** 1746–1754

Yoshimura H, Yanagisawa S, Kanehisa M, Ohmori M (2002) Screening for the target gene of cyanobacterial cAMP receptor protein SYCRP1. Mol Microbiol **43:** 843–853

Zhulin IB, Taylor BL (1998) Correlation of PAS domains with electron transport-associated proteins in completely sequenced microbial genomes. Mol Microbiol **29:** 1522–1523